CHINA'S DUST AFFECTS SOLAR RESOURCE IN THE U.S.: A CASE STUDY

Christian A. Gueymard
2959 Ragis Rd.
Edgewater, FL 32132-2905
e-mail: chris@fsec.ucf.edu

Nels S. Laulainen
Pacific Northwest National Laboratory
Richland, WA
e-mail: nels.laulainen@pnl.gov

Joseph K. Vaughan
Dept. of Civil & Environment. Eng.
Washington State Univ.
Pullman, WA 99164-2910
e-mail: jvaughan@mail.wsu.edu

Frank E. Vignola
Department of Physics
University of Oregon
Eugene, OR 97403-1274
e-mail: fev@darkwing.uoregon.edu

ABSTRACT

The radiative effects of the dust event that hit North America in late April 1998 are studied here as an example of how long-range aerosol transport may temporarily affect the U.S. solar resource. Broadband and spectral radiation data from different sites in the western U.S. are analyzed. At its peak, this event triggered losses of ~30% in beam irradiance and 40% in beam daily irradiation. Considerable effects on the aerosol optical depth at various wavelengths are also reported. Broadband irradiance data were also used to monitor the broadband turbidity during the event. This dust cloud was characterized by a large β turbidity coefficient (up to 0.45) and a very low wavelength exponent, α (0.05–0.2).

Keywords: Aerosols, solar radiation, sunphotometry, turbidity.

1. INTRODUCTION

Geographical, as well as short-term and long-term solar resource variations are mostly caused by variations in cloudiness. Variations in transmission from other atmospheric constituents are typically of secondary importance. However, for solar electric generating technologies that use concentrating collectors, variations in atmospheric transmission have a significant impact. Concentrating systems such as parabolic troughs and solar tower plants utilize only the direct normal beam radiation coming directly from the sun. The more dust and other aerosols in the atmosphere the more the sunlight is scattered and the less beam radiation is available to concentrate. Atmospheric aerosols are known to be the main extinction source of radiation under such cloudless conditions. Aerosols tend to decrease direct radiation but increase diffuse radiation and hence do not affect global radiation nearly as much (e.g., [1]). Earlier studies (e.g., [2, 3]) have shown how a considerable influx of aerosols, such as from the eruption of El Chichón (1982) or Pinatubo (1991), had a long-lasting and adverse effect on solar concentrator systems, precisely because of the significant loss in direct radiation caused by the presence of a thick stratospheric aerosol cloud.

A different type of sudden aerosol influx is examined in this article. The effects of *long-range transport* of desert dust from China on beam irradiance is studied, although forest-fire smoke, or pollution from faraway sources in Asia, South and Central America, or Africa can similarly reduce beam radiation. For instance, it is well known that aeolian dust and sand transport from desert regions of northern Africa (Sahara and Sahel) regularly affects Europe and the Atlantic Ocean. It can adversely affect North and South America as well [4, 5] (see related information at *http://capita.wustl.edu/Databases/UserDomains/SaharaDust2000/).* Smoke clouds from giant forest fires in South and Central America are also detected over the U.S. territory, sometimes causing respiratory problems, and thus health hazards. Dust clouds from Asia regularly affect the Hawaiian Islands each spring [6]. Moreover, it is now realized that the western part of the conterminous U.S. can also be influenced by dust 'storms' originating from China's desert and urban pollutant plumes [7].

The present paper focuses on the potential effect on solar radiation induced by the major desert-dust storm from China that hit the western U.S. in late April 1998. This particular event has the advantage of being recent and well documented. Interestingly, the scientific community was alerted hours before the dust cloud even reached the U.S. and Canada through an interactive website *(http://capita.wustl.edu/Asia-FarEast/).* The results of various investigations devoted to different atmospheric and radiometric aspects of this event are also being published (see, e.g., [8, 9]). The goals of the present contribution are as follows: (i) Quantify the effects of this dust cloud on the solar resource at various sites; (ii) Characterize the radiative importance of this event in terms of turbidity and aerosol optical depth; and (iii) Outline the impact of this event in terms of space and time.

2. BACKGROUND INFORMATION

On April 15-19, 1998 major dust storms occurred in arid areas of northwest China. These were formed by strong cyclonic winds (able to uproot trees) and triggered far-reaching consequences: at first, large yellow dust deposits were dumped over a large part of China, muddy rain occurred in Beijing and other cities as far as Korea, and the winds spread forest fires. These storms resulted in a giant, 1000-km long, dust cloud that passed over Korea and Japan, then crossed the north Pacific to reach the west coast of North America. The peak effect occurred on April 26 at San Nicolas Island and Holtville, CA; April 27 at Eugene and Burns, OR, Boise, ID, Pullman, WA; and April 28 at Davis and Hanford, CA, Desert Rock, NV. The dust cloud was monitored along its journey by different methods, particularly radiometers, lidars, particulate samplers, and satellite pictures [8]. Over the western U.S., many visual observations of strong, unusual, and high-altitude haze were reported from scientists or aircraft pilots, particularly to the website mentioned above. Although it is still difficult to delineate the geographical extent of the dust cloud once it entered North America, it appears from the available radiometric data that Albuquerque and Sevilleta, NM (Fig. 1) were not significantly affected. Low angle satellite photos show that the main body of the cloud moved northeast into Canada. Most radiometric sites with available data eastward of the 105° meridian experienced cloudy weather during the peak period, so that the impact of the dust cloud could not be detected.

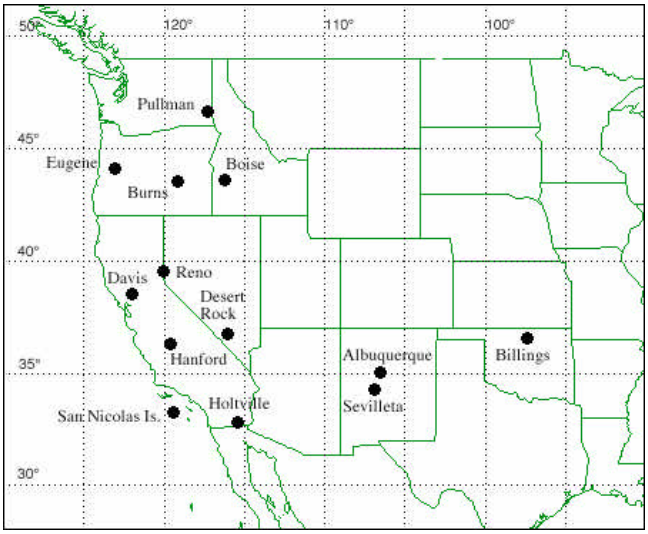

Fig. 1: Map showing the instrumented sites analyzed here.

There is evidence that other 'local' sources of haze were present during the same timeframe, but most probably not at exactly the same time. On one hand, forest fires in Minnesota and the Canadian Rockies, as well as prescribed burns in Oregon, Washington and Idaho, were affecting the northwest U.S. and southern Canada. In another part of the country, huge smoke clouds from forest fires in Guatemala and the Yucatan drifted to the southern U.S. (e.g., Texas). However, the length and geographical extent of the episode make it clear that this Asian dust event was the major source of aerosols affecting a large part of the western U.S. and of southwestern Canada.

Sophisticated instrumentation can be used to detect the physical or chemical signature of each kind of haze, but this is out of the scope of the present study. As far as the solar resource is concerned, any source of haze will produce a noticeable effect on solar radiation, subject of this analysis. Additionally, some spectral characteristics of the particular haze produced by this dust event will be discussed.

3. MEASUREMENTS

The instrumental measurements analyzed here cover the western U.S. where the dust event could be detected and where many solar power plants or other types of solar systems are located. These measurements include direct, diffuse and global broadband irradiance from the University of Oregon's network (averaged at 5-min intervals at Burns and Eugene, OR, 15-min at Boise, ID), similar 3-min data at Desert Rock, NV (from the SURFRAD/NOAA network), 15-min data at Albuquerque, NM and Hanford, CA (from the ISIS/NOAA network), and 3-min data from the USDA network (Davis and Holtville, CA, and Pullman, WA), as well as spectral irradiance data recorded with either a multiple filter rotating shadowband radiometer (MFRSR) or a sunphotometer (SPM) at different sites, and supporting meteorological data. The sites with useful data for this study (i.e., excluding those sites with data gaps or cloudy weather during the peak period) are displayed in Fig. 1.

The radiometric data used here originate from first-class stations with regularly calibrated instruments and sophisticated data quality control. At most sites, direct beam irradiance is measured with a NIP pyrheliometer. Global irradiance is measured with a PSP pyranometer. Diffuse irradiance is normally also measured with a PSP instrument, equipped with either a shadowband or a tracking shading disk. The latter setup is used at first-class research-type sites because of the improved accuracy in diffuse measurement which in turn translates into an accurate—even though indirect— determination of global irradiance (by summing the horizontally-resolved beam irradiance and diffuse irradiance), as discussed elsewhere (e.g., [10, 11]). Boise is equipped with a silicon-based rotating shadowband pyranometer (RSP).

The MFRSR instrument, like the RSP, records global and diffuse irradiance with a silicon sensor, but also the spectral irradiances through narrowband interference filters nominally centered at 415, 500, 615, 670, 870, and 940 nm. Each of these channels, except the last (which is exclusively used to derive precipitable water), provides irradiance data that must be thoroughly analyzed to obtain the aerosol optical depth (AOD) at the corresponding wavelength. For this contribution, the MFRSR data from Eugene, OR and Pullman, WA were analyzed by the third author using an experimental methodology based on [12].

The Cimel SPM, used throughout the AERONET/NASA network, records the beam irradiance behind interference filters, and this is ultimately converted into AODs at 340, 380, 440, 500, 670, 870, and 1020 nm. The SP2-type SPM used at Reno, NV has a single channel at 525 nm, around the peak of visible radiation.

4. EFFECT ON SOLAR IRRADIANCE

Figure 2 exemplifies the typical effect of the intense dust event on direct and diffuse irradiance with data from Boise. The dust cloud was most dense there on day 117 (April 27) with progressive return to approximate normal conditions on day 121. A significant loss in beam radiation at normal incidence is evident (300 W/m^2 or 31% at its peak) with a concomitant increase in diffuse horizontal irradiance that reached ~200 W/m^2 or 310%. The partial redistribution of the lost beam radiation into diffuse radiation results in only a moderate peak loss in global horizontal radiation, of ~45 W/m^2 or 6%. Similar results were obtained at Burns and Eugene, where the peak effect also occurred on day 117.

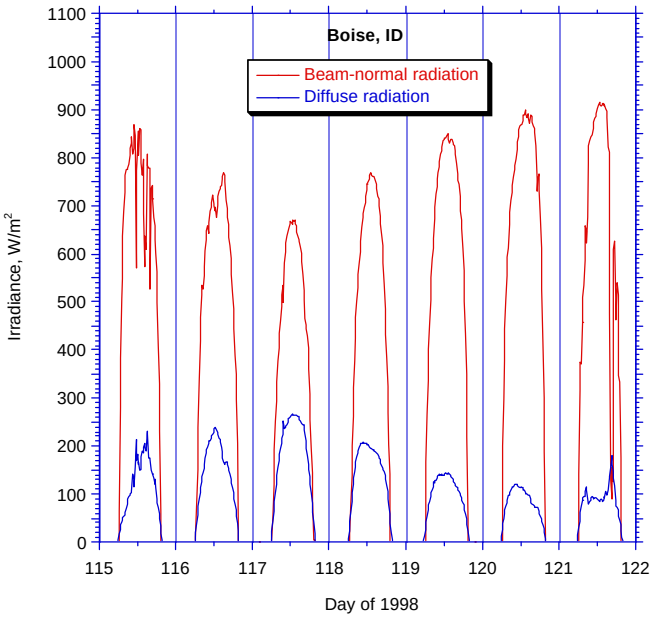

Fig. 2: Beam-normal and diffuse irradiance at Boise, ID for the period covering the dust event of April 1998.

Three common control days (113 and 114 of 1998 and 112 of 1995), for which normal background aerosol conditions were prevalent with no significant cloudiness, were selected for the three sites. The irradiance data from these control days were averaged to obtain both the peak unperturbed irradiances (around solar noon) and the clear daily irradiations. Besides the beam-normal, diffuse and global irradiances, the Eugene site also measures the total irradiances on variously tilted surfaces (only 45°S and 90°S used here as an illustration; the latter is shaded from any ground-reflected radiation) and the UV-A irradiance in the 295–385 nm range. On a daily basis, Table 1 shows that the loss in beam irradiance peaked at more than 40% at all three sites, compared to normal daily totals of 36.9, 39.5, and 41.3 MJ/m^2 at Eugene, Boise, and Burns, respectively. Such a loss translates into a significant impact on solar concentrating devices. Conversely, the overall effect would be much more limited on flat-plate solar collectors or passive solar buildings, with daily global irradiation losses of only 10-11% for tilted surfaces. The ~12% depletion in global UV-A radiation during the peak is essentially attributable to the dust effect because the ozone column was almost conserved.

Because the solar radiation passes through more atmosphere throughout the day than it does at solar noon, when the sun is highest in the sky, the effect on radiation (particularly its beam normal component) is more pronounced on a daily basis than at solar noon. An altitude effect is also apparent, with a gradient of daily losses in beam irradiance from 41% at Eugene (150 m altitude) to 46% at Burns (1265 m altitude). This may be explained by the normally clearer atmosphere at high altitudes caused by a lower background aerosol level and lower precipitable water. The Asia dust cloud was concentrated at a relatively high altitude, between 6 and 10 km [8, 9], so that the variation in aerosol burden was larger (on a relative basis) for a high altitude site (still below the cloud) than for a low altitude site.

TABLE 1: MEASURED RADIATION DURING DAY 117 COMPARED TO NORMAL CONDITIONS

Site	Eugene	Boise	Burns
Altitude (m)	150	701	1265
Noon irradiance (W/m2)			
Beam normal	684 (-27.7%)	671 (-31.0%)	709 (-30.9%)
Global horizontal	867 (-3.8%)	843 (-5.1%)	911 (-4.1%)
Diffuse horizontal	267 (+162%)	268 (+310%)	308 (+328%)
Global 45° south	940 (-9.7%)	-	-
Global 90° south	477 (-10.8%)	-	-
Global UV-A	30.1 (-10.4%)	-	-
Daily irradiation (MJ/m2)			
Beam normal	21.92 (-40.7%	22.34 (-43.5%)	2.19 (-46.2%)
Global horizontal	24.56 (-5.3%	24.27(-6.3%)	5.74 (-5.1%)
Diffuse horizontal	9.48 (+182%)	9.46 (+289%)	0.46 (+373%)
Global 45° south	24.45 (-10.8%	-	-
Global 90° south	11.66 (-9.5%	-	-
Global UV-A	0.81 (-12.3%)	-	-

Another way of interpreting these measurements is to calculate the clear day-solar noon transmittance for beam and global irradiance, K_b and K_T, respectively. The former is a common way of detecting volcanic eruptions. For instance, a study using data from Eugene, Burns, and other sites from the University of Oregon's network showed that the peak decrease in solar-noon K_b reached 20-25% during the first winter after the eruption of El Chichón in 1982 [3]. The same method applied here shows a comparable effect (in magnitude) of the dust cloud on both K_b and K_T, although with a far shorter incidence in terms of duration (Fig. 3).

5. AEROSOL OPTICAL DEPTH AND TURBIDITY

The significant radiative effects just discussed are themselves the consequence of considerable changes in the aerosol content of the local atmosphere. Documenting the variations in turbidity at different sites supplies critical information that improves the performance of solar radiation models [13].

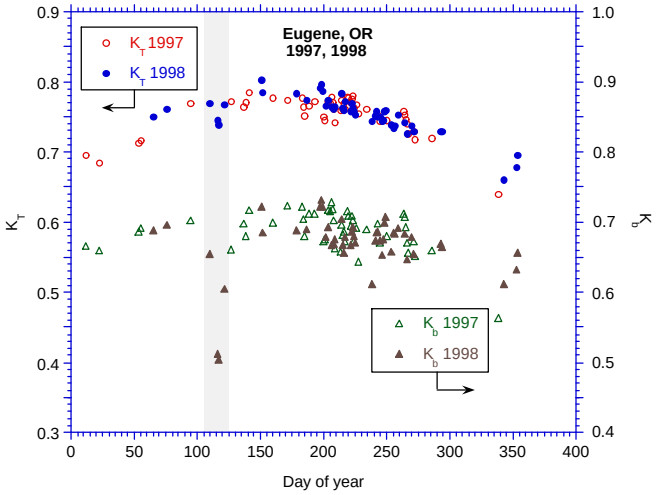

Fig. 3: Clear-day solar-noon beam and global transmittance, K_b and K_T, at Eugene, OR for 1997 and 1998.

When using an MFRSR or a multiwavelength SPM, it is possible to derive the Ångström turbidity coefficient ß and the wavelength exponent, a, by fitting the spectral AODs from each scan, d_{a1}, to the classic Ångström equation:

$$d_{a1} = ß\ l^{-a} \qquad (1)$$

Coefficient ß is a common measure of the total aerosol loading of the atmosphere, whereas a, which is linked to the average size of the aerosol particles, is an easy conventional way of describing the aerosol spectral extinction behavior, through Eq. (1).

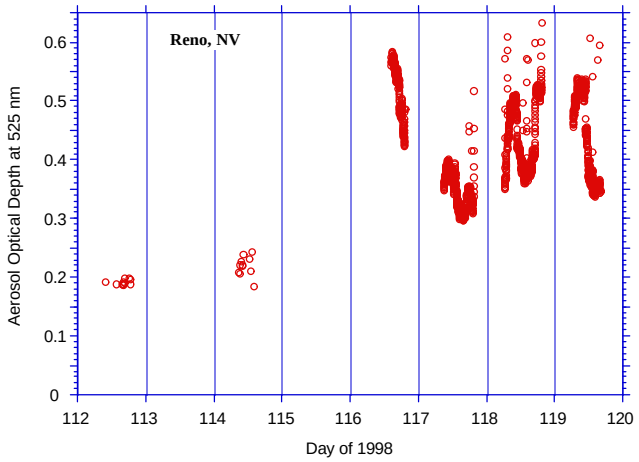

Fig. 4: Variation of the AOD at 525 nm recorded with a sunphotometer during the dust event at Reno, NV.

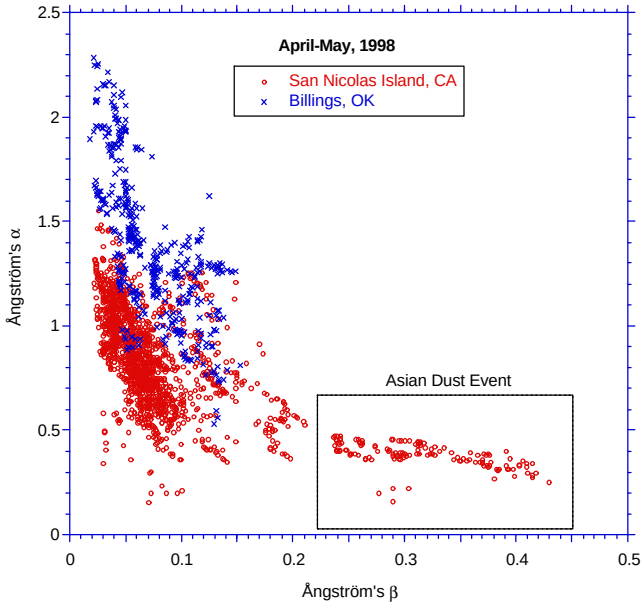

Fig. 5: Inverse relationship between a and ß at Billings, OK and San Nicolas Island, CA.

Alternatively, ß can be estimated from broadband irradiance data if a is fixed at 1.3, the conventional value that corresponds to the frequent case of rural aerosols. For this investigation, both the direct beam method [14] and the diffuse-beam ratio method [10] are used wherever possible.
Furthermore, these two methods also calculate the broadband-average AOD, d_a , which is the turbidity input for different solar radiation models (e.g., [15]). It has been shown [16] that d_a is equivalent to d_{a1} for a key wavelength, which is normally in the 700–850 nm range, thus providing some basic spectral information from inexpensive and more widely available broadband radiation data. The datasets assembled here offer an ideal opportunity to investigate to which extent these broadband turbidity methods are applicable to such an exceptional case (of severe atmospheric loading with aerosols of non-rural origin), by comparison with more detailed data provided by the spectral instruments. Fortunately, networks or sites equipped with such are expanding. For the present study, clear-sky spectral data from Davis, Holtville, and San Nicolas Island, CA, Eugene, OR, Reno, NV, Pullman, WA, and Billings, OK could be obtained. The latter site is ~2200 km from the west coast (Fig. 1) and is used here as a control site, with a typical rural aerosol environment. It is possible that the dust cloud passed over this site, but the weather was cloudy at that time. The AOD there was only marginally higher than normal on April 30.

The largest increase in visible AOD is observed at Reno, where a single-channel SPM was deployed just prior to the dust event (Fig. 4). Compared to the background AOD of the previous days, it can be inferred that the overburden in optical depth caused by the dust cloud was about 0.45 at 525 nm.

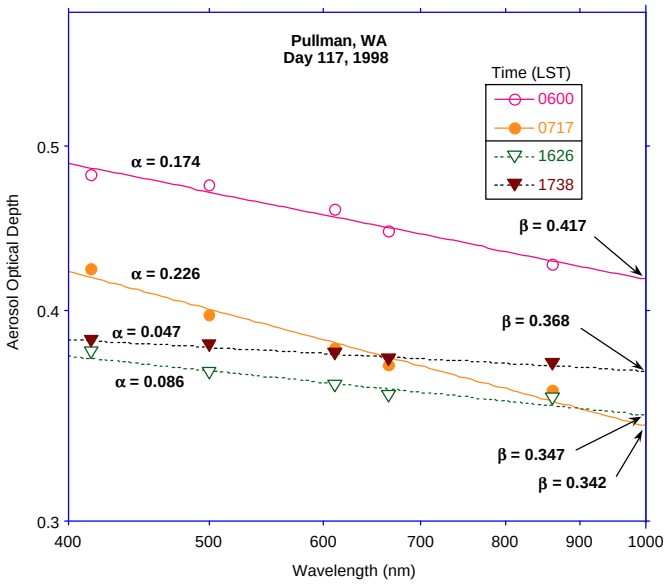

Fig. 6: Spectral AOD *vs* wavelength during the peak dust event day for Pullman, WA.

For sites that are equipped with multispectral instruments, the coefficients a and ß can be obtained by regression through Eq. (1). It is particularly informative to study the time variations of both coefficients. Figure 5 shows that they tend to vary in opposite directions from each other, both at the maritime site of San Nicolas Island and the rural site of Billings. Because maritime aerosols tend to be of larger size than rural aerosols, the background a is generally lower at San Nicolas. However, the dust cloud episode is clearly characterized by very low a (down to 0.2) and very high ß values (up to 0.5). The same observation also applies to results from Eugene and Pullman (from the SIRN/GISS and USDA networks), where spectral AODs for AM and PM periods were determined by a method based on the objective Langley algorithm approach [12]. Langley retrievals for top-of-atmosphere (TOA) irradiances were filtered, based on the ratio-Langley method [17]. Resulting TOA irradiances were used with the Bouguer-Lambert-Beer law to find improved estimates for AODs. Figure 6 shows a characteristic Ångström plot with which the AODs are fitted to Eq. (1) to obtain both a and ß. Selected AM and PM data of the peak day (April 27) at Pullman are shown here, including the records of maximum ß, 0.417 (at 06:00 LST) and minimum a, 0.047 (at 17:38 LST). Therefore, the decrease in a is even more pronounced there than at San Nicolas, whereas the peak ß is approximately the same at both sites.

In terms of either ß or the 500-nm AOD, the overburden caused by the dust cloud can be estimated at 0.35–0.40 at Eugene, Pullman and San Nicolas. Using broadband direct beam irradiance data, the overburden in terms of broadband average AOD is also ~0.4 at Eugene and Pullman.

Because a is so low, the broadband turbidity methods that are based on the rural aerosol hypothesis (a=1.3) cannot estimate ß correctly. However, at sites where spectral instruments are not available, these methods are still valuable and provide a 'reduced' value of ß, noted ß*, that is useful in detecting deviations from normal seasonal variations in turbidity, or occasional events caused by volcanic eruptions [18, 19]. A comparison between the estimated ß* (with the direct-beam method [14]) at Eugene, Holtville and Desert Rock during the dust event appears in Fig. 7, showing notable site-to-site differences in turbidity and its daily variations. The peak loss in beam irradiance was significantly less at Holtville (10%) and at Desert Rock (8%), compared to the 28% lost at Eugene.

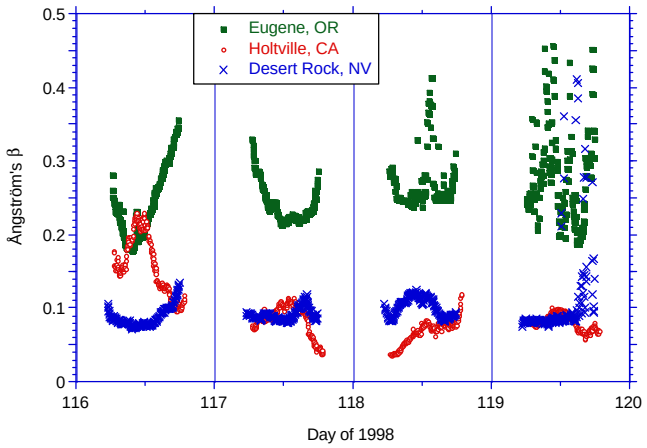

Fig. 7: Reduced ß turbidity coefficient, ß*, for a=1.3 (from broadband beam irradiance data) at different sites.

A preliminary comparison of the broadband AOD (using the direct-beam method [14]) and the spectral AOD at 673 and 868 nm from Eugene's MFRSR appears in Fig. 8. Even though the spectral results are not complete for that day, Fig. 8 clearly shows that the broadband AOD can be approximated by the spectral AOD at some wavelength between 673 and 868 nm, thus experimentally confirming the global validity of the broadband-spectral equivalence discussed in [16], at least for the present conditions.

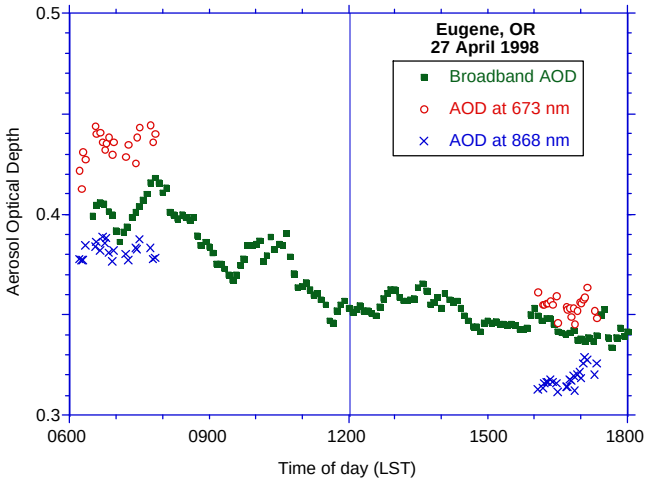

Fig. 8: Broadband *vs* spectral AOD during the peak dust event day at Eugene, OR.

Finally, it appears from Figs. 4, 5, 7 and 8 that variations in daily turbidity and AOD are extremely rapid during such a dust

event, like variations in cloudiness during a thunderstorm. This feature is not obvious when looking at irradiance records only.

6. CONCLUSION

The radiative effect of intense dust or smoke events such as the Asian dust event of 1998 studied here is relatively short-lived (a few days) compared to large volcanic eruptions, but it has a similar radiative intensity and signature, characterized by a large Ångström's turbidity coefficient, $ß$, and a very low wavelength exponent, a, with a clear inverse relationship between them. At its peak, this event triggered losses of ~30% in beam irradiance and 40% in beam daily irradiation. The average aerosol optical depth, calculated from broadband irradiance data, had a peak at ~0.6 at many sites, or ~6 times the normal value for that period.

It is recommended that events of this kind be studied more closely in relation with the U.S. solar resource because: (i) the occurrence of these U.S.-bound dust events from Asia is concentrated during a single season (Spring) due to favorable atmospheric conditions; (ii) the impact of these pollutant plumes may increase in the future because of the rapid growth in agriculture and the growing use of inefficient coal-fired plants in Asia; (iii) such dust events have demonstrable radiative effects, particularly on beam irradiance and turbidity; (iv) they may combine with outbreaks of dust clouds from other regions (e.g., forest fires) and (v) they have a definite social and economic impact.

7. ACKNOWLEDGMENTS

CAG thanks David W. DuBois who kindly provided his data for Reno, Jim Slusser for the MFRSR data from the USDA UV-B network. Robert Frouin and Rangasayi Halthore kindly gave him permission to use their Aeronet data.

NSL has been supported by the U.S. Department of Energy (DOE) under Contract DE-AC06-76RLO 1830. Pacific Northwest National Laboratory is operated for DOE by Battelle Memorial Institute.

JKV thanks the Columbia Plateau PM-10 Program for support and Dave Bigelow of the USDA UV-B Radiation Monitoring Program for help with the Pullman data.

FEV thanks Izabela Santos for help gathering the Eugene MFR data, and acknowledges support from the Regional Solar Radiation Data Monitoring Consortium (Eugene Water and Electric Board, Bonneville Power Administration, Northwest Power Planning Council, Portland General Electric, PacifiCorp, and the National Renewable Energy Laboratory), and the Goddard Institute of Space Science.

8. REFERENCES

(1) Gueymard, C., A two-band model for the calculation of clear sky solar irradiance, illuminance, and photosynthetically active radiation at the Earth's surface, *Solar Energy*, **43**, 253-265 (1989).

(2) Michalsky, J.J., et al., Degradation of solar concentrator performance in the aftermath of Mt Pinatubo, *Solar Energy*, **52**, 205-213 (1994).

(3) Vignola, F. and D.K. McDaniels, *Effects of El Chichón on global correlations*, Proc. ISES Conf., Intersol 85, 2434-2438 (1986).

(4) Prospero, J.M., Long-term measurements of the transport of African mineral dust to the southeastern United States: Implications for regional air quality, *J. Geophys. Res.*, **104D**, 15,917-15,927 (1999).

(5) Swap, R., et al., Temporal and spatial characteristics of Saharan dust outbreaks, *J. Geophys. Res.*, **101D**, 4205-4220 (1996).

(6) Perry, K.D., et al., Long-range transport of anthropogenic aerosols to the National Oceanic and Atmospheric Administration baseline station at Mauna Loa Observatory, Hawaii, *J. Geophys. Res.*, **104D**, 18,521-18,533 (1999).

(7) Jaffe, D., et al., transport of Asian air pollution to North America, *Geophys. Res. Lett.*, **26**, 711-714 (1999).

(8) Husar, R.B., et al., The Asian dust events of April 1998, *J. Geophys. Res. (in press)* (2000).

(9) Tratt, D.M., et al., The April 1998 Asian dust event: a Southern California perspective, *J. Geophys. Res. (in press)* (2000).

(10) Gueymard, C. and F. Vignola, Determination of atmospheric turbidity from the diffuse-beam broadband irradiance ratio, *Solar Energy*, **63**, 135-146 (1998).

(11) Michalsky, J., et al., Optimal measurement of surface shortwave irradiance using current instrumentation, *J. Atmos. Ocean Technol.*, **16**, 55-69 (1999).

(12) Harrison, L. and J. Michalsky, Objective algorithms for the retrieval of optical depths from ground-based measurements, *Appl. Opt.*, **33**, (1994).

(13) Gueymard, C., Critical analysis and performance assessment of clear sky solar irradiance models using theoretical and measured data, *Solar Energy*, **51**, 121-138 (1993).

(14) Gueymard, C., Turbidity determination from broadband irradiance measurements: A detailed multicoefficient approach, *J. Appl. Meteorol.*, **37**, 414-435 (1998).

(15) Maxwell, E.L., METSTAT—The solar radiation model used in the production of the National Solar Radiation Data Base (NSRDB), *Solar Energy*, **62**, 263-279 (1998)

(16) Molineaux, B., et al., Equivalence of pyrheliometric and monochromatic aerosol optical depths at a single key wavelength, *Appl. Opt.*, **37**, 7008-7018 (1998).

(17) Forgan, B.W., Sunphotometer calibration by the ratio-Langley method. *Baseline Atmospheric Program 1986*, B.W. Forgan and P.J. Fraser, eds. (Bureau of Meteorology, Melbourne, Australia), pp. 22-26 (1988).

(18) Gueymard, C., Analysis of monthly average atmospheric precipitable water and turbidity in Canada and Northern United States, *Solar Energy*, **53**, 57-71 (1994)

(19) Gueymard, C. and J.D. Garrison, Critical evaluation of precipitable water and atmospheric turbidity in Canada using measured hourly solar irradiance, *Solar Energy*, **62**, 291-307 (1998).